Proceedings of the ASME 2019 38th International Conference on Ocean, Offshore and Arctic Engineering
OMAE2019
June 9-14, 2019, Glasgow, Scotland, UK

OMAE2019-95244

COUPLED NUMERICAL ANALYSIS OF A CONCEPT TLB TYPE FLOATING OFFSHORE WIND TURBINE

Iman Ramzanpoor, Martin Nuernberg, Longbin Tao
Department of Naval Architecture, Ocean and Marine Engineering,
Strathclyde University
Glasgow, G4 0LZ, UK

Abstract

The main drivers for the continued decarbonisation of the global energy market are renewable energy sources. Moreover, the leading technological solutions to achieve this are offshore wind turbines. As installed capacity has been increasing rapidly and shallow water near shore sites are exhausted, projects will need to be developed further from shore and often in deeper waters, which will pose greater technical challenges and constrain efforts to reduce costs.

Current floating platform solutions such as the spar and semi-submersible rely on large amounts of ballast and complex structural designs with active stabilisation systems for stability of the floating offshore wind turbine platform (FOWT).

The primary focus of this study is to present a design concept and mooring arrangement for an alternative floating platform solution that places emphasis on the mooring system to achieve stability for a FOWT. The tension leg buoy (TLB) is designed to support future 10MW offshore wind turbine generators.

This paper presents the numerical methodology used for a coupled hydro-elastic analysis of the floater and mooring system under combined wind, wave and current effects.

A concept TLB design is presented and its platform motion and mooring line tension characteristics are analysed for a three-hour time domain simulation representing operating and survival conditions in the northern North Sea with water depths of 110 metres. The importance of wave drift forces and the other non-linear excitation forces in the concept design stage are evaluated by comparing the motion and tension responses of three different numerical simulation cases with increasing numerical complexity.

The preliminary TLB system design demonstrated satisfactory motion response for the operation of a FOWT and survival in a 100-year storm condition. The results show that accounting for second-order effect is vital in terms of having a clear understanding of the full behaviour of the system and the detailed response characteristics in operational and survival conditions. Extreme loads are significantly reduced when accounting for the second-order effects. This can be a key aspect to not overdesign the system and consequently achieve significant cost savings.

Keywords: Floating Wind, Tension Leg Buoy, Second Order Wave Forces

INTRODUCTION

According to Wind Europe [1], floating offshore wind turbine (FOWT) technology holds the key to using an inexhaustible resource potential in Europe. It is estimated that approximately 80% of the offshore wind resource is located in water depths of 60m and beyond where traditional bottom fixed offshore wind is not economically appealing [2]. The European wind energy association (EWEA) anticipated 40GW offshore wind capacity could be operating in European waters, proceeding 148TWh by 2020 when offshore wind is expected to account for 30% of the new annual installation within the wind industry [3]. The UK has an opportunity to build on being in a world leading position and develop supply chain capability to exploit opportunities in international markets, as there is a potential for up to 90MW to be installed by 2018 [4].

Although the vision for large-scale FOWT was introduced by Professor William E. Heronemus at the University of Massachusetts in 1972, it was not until the mid-1990's, after the commercial wind industry was well established, the topic was considered again by the research community [5]. A semi-submersible type FOWT called WindFloat with a 2MW turbine was constructed and installed in 2011 and subsequently , Phase 2 Wind Float pre-commercial project aims for a total capacity of 25MW using 3 MVOW'sV164 Turbine (8MW) to be deployed in 85-100 m water depth [6, 7]. Hywind Scotland is the world first full-scale SPAR-type FOWT structure and wind farm with 6 MW turbines which were installed in 2017 in Scotland with total capacity of 30MW [8-10]. After the nuclear disaster in Japan in 2011, the Japanese government started to construct and deploy large scale FOWTs [11]. Fukushima offshore wind consortium is proceeding with Fukushima floating offshore wind farm demonstration project funded by the ministry of economy, trade and industry [12]. The first phase of the Fukushima FORWARD project consists of the 2MW floating wind turbine, which was the world first 25MVA floating substation and submarine cable, was completed in 2013. According to Fukushima offshore wind consortium, the second phase of the project the world largest 7MW floating wind turbine (V-shape Semi-Sub) and 5MW floating wind turbine (Advanced Spar) were intended to be installed in 2014 and 2015 respectively. They were successfully installed in 2015 and 2016 instead. [13].

The current key challenge in the FOWT industry and research is designing economically efficient floating systems that can compete with fixed-bottom offshore turbines in terms of levelized cost of energy (LCOE) [14]. Due to the infant nature of the industry, detailed analysis of the coupled response of the wind turbine, floating platform and mooring system is a key aspect in achieving significant cost savings and ensuring safe and reliable performance of the whole system. As deep-water offshore designs are at an early stage of development, modelling the integration of wind turbine with the deep-water FOWT platform is one of the important issues that has a significant impact on project costs [15]. Construction and installation methods of FOWT units have shown to still require further optimisation, and cost reduction before FOWT farms can be constructed at large scale [16]. However, specific issues such as vibration, complex operating parameters and limited equipment lifetime will escalate technical and economic challenges in wind farm operation (wake effects, yield and power output) and require integrated modelling tools to understand advanced materials, loads and limitations of mooring system to optimise installation process. These are represented mostly through reliability, accessibility and logistics issues as well as specialised vessel deployment costs. This can be a result of selecting wrong turbine, blade or substation materials, improper design and installation and would result in a shorter lifetime, lower safety and higher maintenance costs for the offshore wind power system [17].

While previous designs rely on large amounts of solid ballast (Hywind Spar) that take several weeks to be installed in the floating platforms, or have developed complex ballasting systems (WindFloat) and improved wind turbine control systems to reduce the overall motion response of the floating platform, improved performance and reliability along with a design and installation method that takes large scale deployment into account can be achieved by placing emphasis on the mooring system from the outset of the design process.

The aim of this project is to deploy FOWT in the North Sea by taking into account the limitation for land based construction infrastructure due to size and water depth limitations of ship yards and harbours and cost as well as time consideration of installation and maintenance given the distance from shore to offshore wind farms and requirement for large vessels during installation. A technically and economically sound maintenance procedure using for example a maintenance at sea approach could also significantly reduce the lifetime cost of large scale offshore floating wind farms.

In 2014, Marine Scotland identified seven Regional Locational Guidance Options (RLGOs) for deep water floating wind technologies. These sites were identified as potentially low risk locations for site evaluation and potential project development ranging in depths from 36m (West of Colonsay) to 120m (East of Shetland and Southeast of Aberdeen) [18].

The 10MW TLB-FOWT platform presented in this study relies on excess buoyancy and mooring stiffness to provide the required stability for operation of the wind turbine and survival in extreme North Sea conditions at 110m water depth. The TLB platform modelled in this paper is developed based on the TLB concept proposed by Sclavonous [19] and later by Myhr [20, 21]. The wind turbine adapted for this project is the DTU 10MW reference turbine [22-24] and dimensions of the initial TLB concept have been adapted for the increased load of the 10MW generator. One of the advantages of the TLB is that it could adapt complex installation procedures in comparison to the complex vertical configuration of the TLP system and the spar where ballasting operations are very time consuming. The other advantage of TLB compared with Spar Platform is the reduction in draft and overall material cost. For instance, Hywind 6MW has approximately 95m draft [25] whereas the TLB modelled for this study has 62m draft.

The most significant components of the FOWT motion response are those in the wave frequency range for all translational and rotational motion. Nonlinear excitation such as sum and difference frequency combinations can also have significant effects on the motion response at various degrees of freedom, which will influence the mooring line forces significantly. Due to their increased computational demands and complexity, preliminary design of offshore structures often neglects the higher order forces as these are assumed to be at least an order of magnitude smaller than the first order forces. It was previously shown Previous study [26] showed that the second order forces for TLP type floating offshore wind turbines are significantly higher than that for spar platform with catenary mooring, and they can be of the same magnitude as the first order forces. The sum frequency dominated the response in heave whereas the difference frequency dominated in the surge response of the TLP. These simulations however neglected effects due to viscous drag, which could be significant for the slender parts of the TLP tested.

Therefore, in this study, the first and second-order wave forces, added mass and radiation damping will be computed based on potential theory in the hydrodynamic analysis code WADAM, which is integrated through HydroD into the DNVGL SESAM software package. The coupled motion response of the TLB system in defined environments for operating and storm conditions will be calculated using SIMO/RIFLEX in SESAM's DeepC program allowing for excitation force, motion response and mooring line response calculations.

This project will be focusing on presenting the results of a concept development study for a TLB type FOWT in operating and storm conditions The importance of wave drift forces and second-order wave forces on the coupled hydrodynamic response is demonstrated for both conditions thus providing important insights and improvements to the concept development methodology for floating offshore wind turbines of similar type prior to including a more detailed representation of the forces induced by operation of a fully modelled wind turbine generator.

The paper first introduces the numerical methodology applied to determine the coupled response for the floater and mooring system under wind, wave and current effects before the design parameters of the concept floater and mooring line are presented along with the detailed environmental conditions used

to evaluate the performance of the FOWT design. Results are presented for calculation of the response using a first-order linear approach, first-order and wave drift forces and a second-order approach. Finally, the conclusions of this preliminary concept design study are presented and further work for the detailed development and analysis of an alternative FOWT system are highlighted.

1. THEORETICAL AND NUMERICAL MODELLING

DNV-GL WADAM (Wave Analysis by Diffraction and Morison Theory) is used for frequency domain hydrodynamic analysis [27]. The frequency domain hydrodynamic analysis is performed without the mooring lines directly. The resulting mooring system stiffness however, is applied to the calculations. Forces and moments are taken into account in terms of transfer functions. Added mass and radiation damping of hydrodynamic coefficients, wave excitation forces, and response operators are calculated in WADAM, solved by potential theory based on the implementation of 3D panel method and Green's theorem in WAMIT [28]. The coupled motion response of floating platforms and mooring lines is computed in time domain in SIMO-RIFLEX to provide results for the dynamic response in terms of motion and mooring forces.

1.1 POTENTIAL THEORY

By assuming incompressible, irrotational flow, the fluid velocity vector can be defined as the gradient of the total velocity potential Φ, satisfying the Laplace equation:

$$\nabla^2 \Phi = 0 \qquad \text{(Eq.1)}$$

The complex velocity potentials can be expressed in terms of incident wave (I), diffracted wave (D) and wave radiation (R). This is based on the linearity assumption. The product of all complex quantities with the factor e^{iwt} applies due to the harmonic time dependence.

Based on a non-dimensional perturbation parameter, ε, higher order terms can be included. Therefore, the boundary value problem (BVP) can be defined by using;

$$\Phi = \Phi_I + \Phi_D + \Phi_R \qquad \text{(Eq.2)}$$

$$\Phi_I = \sum_{n=1}^{\infty} \varepsilon^n \Phi_n \qquad \text{(Eq.3)}$$

$$\Phi_R = i\omega \sum_j \xi_j \Phi_j \qquad \text{(Eq.4)}$$

Where ω represents the wave frequency, t is time, ε is the perturbation, n is the desired order of the solution, ξ is the amplitude of motion for each degree of freedom j. The diffraction potential is computed using an additional radiation boundary condition to account for the vanishing effect at great distance from the structure [29].

Inclusion of non-linear forces acting on floating platforms increased the computational demands significantly and is therefore often neglected at early design stages. While smaller in magnitude, sum and difference frequency may excite a structures' natural frequency above and below the frequency of the first order forces. This can result in large slow oscillations or high frequency vibrations in systems where difference or sum frequencies respectively are significant.

The second order forces from the diffraction problem are split into contributions due to the quadratic interactions from first order terms on the body and free surface (F_q) and the second order velocity potential (F_p) as shown in (Eq. 5). The total excitation forces used to calculate the motion response of the floating structure include both, the first order and second order forces. The second order velocity potential accounting for the interaction between two harmonically oscillating components such as two incident linear waves or a wave and body oscillating at first order frequency is defined in (Eq. 6) :

$$F_{ex}^{(2)} = F_p + F_q \qquad \text{(Eq.5)}$$

$$\Phi^{(2)}(\bar{x}, t) = Re \sum_k \sum_l \Phi_{kl}^{+} e^{i(\omega_k + \omega_l)t} + \Phi_{kl}^{-} e^{i(\omega_k - \omega_l)t} \qquad \text{(Eq. 6)}$$

Where Φ_{kl}^{+} and Φ_{kl}^{-} are the velocity potentials at the sum frequencies $(\omega_k + \omega_l)$ and difference frequencies $(\omega_k - \omega_l)$, as described by Roald et al. [30].

Within the SESAM software package, the panel model accounts for the hydrodynamic loads and a mass model can be used to account for global mass distribution and inertia of the platform. In this study, the mass of the wind turbine including rotor, nacelle, hub and tower are included with their respective centre of gravity. The HydroD module is a graphical user interface (GUI) and responsible for running the first-order and second-order hydrodynamic analysis using WADAM as a solver. Hydrodynamic analysis schematic using WADAM is presented by Md Touhidul Islam [31]. 3D Potential theory for first and second order hydrodynamics in WADAM are based on WAMIT [28]. Time domain analysis can then be performed in DeepC or Sima using SIMO/RIFLEX to obtain results for coupled floater and mooring system response.

The basic part of a panel model consists of quadrilateral or triangular panels representing the wet surfaces of a body. By discretizing the wetted surface of the structure into a number of panels, integral equations are used to set up a system of simultaneous equations to be solved for the velocity potentials. Constant radiation and diffraction potentials across these panels are assumed and the hydrodynamic pressure on the structure as well as calculations of added mass and radiation damping are obtained.

Taking into account the excitation forces, the resulting added mass and potential damping matrices and response amplitude operators up to second-order in combination with the wave, wind and current excitation forces as well as the floating platforms' mooring configuration allows for computing the motion response and mooring line loads in the time domain analysis in DeepC.

The equations of motions can be written in the form of Newton's second law. The generalised force vector (Eq.7) includes all the environmental forces such as inertial and gravitational forces, mooring system and soil interaction (if applicable), and all kind of stiffness and damping forces (including aerodynamic, hydrodynamic and structural stiffness and damping).

$$F = F_{Hydrodynamic} + F_{Aerodynamic} + F_{Mooring\ System} + F_{Gravitional} + \cdots \quad \text{(Eq.7)}$$

In this study, $F_{Hydrodynamic}$ includes the first order wave excitation forces, first order and horizontal wave drift forces and the combined first and second order wave excitation forces respectively for the presented cases calculated in WADAM. Additionally, $F_{Aerodynamic}$ is represented through mean thrust forces accounting for the operation of the turbine or the drag acting on the turbine support structure when the system is not operational. $F_{Mooring}$ accounts for the mooring system forces acting on the floating support structure.

The equations of motion for a floating wind turbine (Eq.8) are nonlinear and can be solved in the time domain using direct step-by-step integration techniques. Time domain analysis allows the handling of nonlinearities involved in hydrodynamic and aerodynamic loading and finite wave amplitude effects as well as nonlinear material and geometrical effects.

$$F(t, X, \dot{X}) = (m + A_\infty)\ddot{X} + (D_{Hydro1} + D_{Aero1})\dot{X} + (D_{Hydro2} g_{hydro} + D_{Aero2} g_{Aero}) + KX \quad \text{(Eq.8)}$$

where m is the body mass matrix, A is the frequency-dependent added mass matrix, D_{Hydro1} is the linear viscous hydrodynamic damping matrix, D_{Hydro2} is the quadratic viscous hydrodynamic damping matrix, D_{Aero1} is the linear aerodynamic damping matrix, g_{hydro} and g_{Aero} are vector functions where each element is given by $g_i = \dot{X}_i|\dot{X}_i|$, K is the position-dependent hydrostatic stiffness matrix, x is the position vector including translations and rotations.

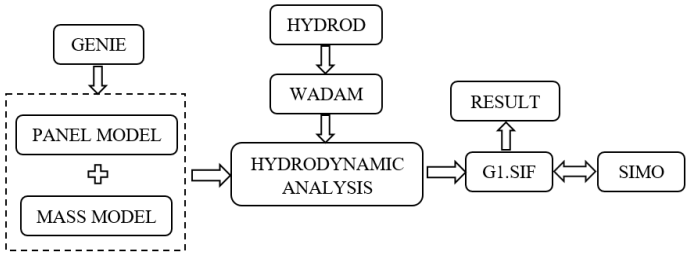

Figure 1: Hydrodynamic Computing Flowchart (Source: Islam [31]).

The hydrodynamic analysis is conducted for three separate cases with increasing computational complexity and requirements. Firstly, only first order wave excitation forces are considered for the coupled dynamic analysis. Secondly, the first order wave excitation plus horizontal wave drift computed based on far field integration using momentum conservation are used. Finally, the combined first and second order wave excitation forces are used for the coupled dynamic analysis of the TLB floater and mooring system.

A mesh convergence study was performed and the final panel model of the floating structure consisting of 2502 elements per quarter as two planes of symmetry were used to reduce computational effort. Further, the second-order free surface mesh required to calculate the second-order velocity potential was modelled to consist of 1250 elements per quarter.

2. FOWT PLATFORM & WIND TURBINE

Currently, the main cost factor of a FOWT system is the support platform. The structural design has a significant influence on the technical design of sub-systems such as ballasting and mooring equipment required and determines the cost-effective feasibility of the system.

As the development in the wind power industry strives towards larger wind turbines, the scientific community also needs a comparable standard for a 10MW wind turbine. The DTU 10MW Reference Wind Turbine (DTU 10MW RWT) was developed to serve this purpose. The development of the 10MW reference turbine started with the efforts to develop new rotor designs in the "Light Rotor project" [32]. This development only covers the details for a turbine based onshore; therefore, the tower characteristics of the onshore design have to be adjusted for the application on the floating platform by shortening the total tower length to fit between the top of the floater (at 20m above sea level) to the underside of the nacelle (at 116m above sea level). This can be achieved either by the ratio of the tower masses or by the height ratio [33].

The most important consideration in scaling the floating platform from previous studies [20] is ensuring its excess buoyancy levels remain sufficient for the system to achieve stability.

Table 1: Overview of FOWT Properties

TLB 10MW FOWT Properties	
Draft	62m
Diameter SWL	20m
Diameter Bottom	20m
Mass	1324t
Centre of Gravity	28.22m
Hub Height Turbine	119m
Rated wind speed	11.4m/s
Rotor Diameter	178.3m

The platform excess buoyancy and mooring stiffness is gradually increased through varying platform dimension and mooring line radius to ensure acceptable motion and mooring performance for the coupled system in operational and survival conditions. For the initial model, the ratio between excess buoyancy and weight is kept approximately constant between 5MW and 10MW model, however extensive simulations and design iterations are then completed with additional design modifications.

The preliminary design that led to both, low motions and tensions in operating condition and successful survival of an extreme event is presented in this section. A schematic layout is shown in Figure 2 and main properties of the TLB design concept are given in Table 1.

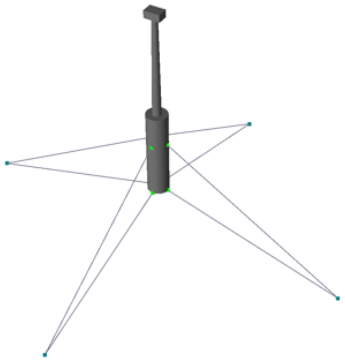

Figure 2: Schematic view of TLB 10MW FOWT.

2.1 MOORING SYSTEM

The mooring system applied to the TLB is similar to that presented in Trolle and Hornbak [34], however a considerably larger anchor radius is used to give the opportunity for anchor sharing when located in a farm of multiple floating wind turbines which will be investigated following the successful design of the concept floater. The mooring system consists of eight mooring lines in total, distributed in two clusters of lines at 90° angles. The mooring lines are attached at two heights, one at the bottom of the floater with angle of attachment of 19° and one 10m below SWL with angle of attachment of 30° to give sufficient clearance with regards to the fairlead location and free surface and maneuvering of vessels near the platform (Figure 3).

The initial anchor radius is set to 180m. A spiral strand mooring line is assumed for this initial concept test with a mooring line radius of 0.243m and a Young's modulus of 207GPa. The axial stiffness of the line is calculated using Eq.7 [35].

$$Axial\ Stiffness = \begin{cases} 3.67E+7\ d^2 & Fibre\ Core \\ 4.04E+7d^2 & Wire\ Core \end{cases} \quad \text{(Eq.7)}$$

The description of the mooring layout is presented in Table 2. The stiffness matrix of a mooring system composed of multiple lines is evaluated by summing the stiffness matrices of the individual lines following the procedure presented in [36]. As in the case of taut-leg mooring system, where the line does not contact the seabed and is taut due to the pretension which caused by the platform excess buoyancy, most of the restoring loads are generated by line elasticity. The lines are inclined (with angle) and the anchor experiences horizontal and vertical loads. While a single attachment point is modelled, a yaw stiffness is included in the global stiffness matrix that has been approximated based on the methodology presented in [36] for an assumed 20 degree spread of the attachment point to replicate the effects of a bridle/delta connection to reduce the yaw motion of the platform.

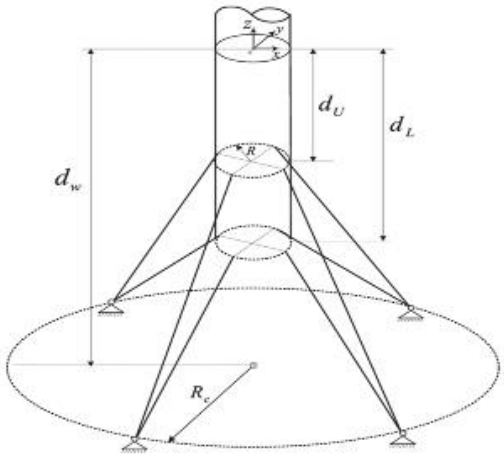

Figure 3: Four anchor taut-leg floating wind turbine Concept. (Source: Alsolihat [36])

Table 2: Mooring Layout

No. of Lines	2 sets of 4 lines
Angle between Lines	90°
Radius Plat. CL to Anchor	180m
Fairlead below SWL	-10m & -62m

2.2 Environmental Conditions

Characterisation of the existing physical environment and sediment processes for potential deployment sites is based on both existing and site-specific survey data. Floating solutions are expected to be cost efficient for water depth greater than 60m [37] however this number varies for each concept design and different technical solutions may be favourable for different locations based on their mooring characteristics and motion behaviour.

In the scope of this study, a water depth of 110m is considered, approximately representing the location of the Hywind Scotland floating wind turbine demonstration wind farm. In this study, two scenarios of environment conditions are defined based on the location of deployment. Firstly, an operational condition (OC) and secondly a survival condition (SC) representing the extreme event of a 100 year return period wave event. For the environmental load cases presented here, it is assumed that wind wave and current are co-linear and the direction is set to be in line with mooring line 1 and line 4.

The current profile is based on current measurements at the deployment location of the Hywind Scotland Floating Wind farm with maximum current velocities of 0.4m/s and 1.42m/s for operation and storm condition respectively.

The wave and current conditions used for the motion response analysis of both scenarios are shown in Table 3. According to ORECCA-RSE (Off-shore Renewable Energy Conversion platforms - Coordination Action), most areas of the North Sea around the Scotland shore have depths between 60m

to 200m, with slightly deeper trenches of up to 500m depths. As several projects are planned or under construction at around 300km offshore, it can be assumed that the cost for operation and maintenance as well as connection costs are within a reasonable scope for a maximum distance to shore of 300km [38].

For operational condition of the 10MW DTU turbine, the rated wind speed of 11.4m/s is considered. For the initial concept design, the wind force is assumed to be acting as a static thrust force on the hub of the turbine, defined in terms of the area swept by the rotor and the rated operating wind velocity and a thrust coefficient as presented in Table 3. For the survival condition, the wind speed of 40m/s is considered, however due to the rotor not being operational, the SC wind force applied as a constant force estimated from the projected area and a drag coefficient.

Table 3: Environmental Conditions

Environmental Conditions	Operation	Storm
Water Depth	110m	
Significant Wave Height (H_S)	4m	19.7 m
Peak Period	7s	13.2 s
Wave heading	180°	
Wind speed at Hub	11.4 m/s	40 m/s
Thrust coefficient	0.78	
Maximum Current	0.4 m/s	1.42 m/s

3. RESULTS & DISCUSSION

All time domain simulations are run for a three-hour time duration. Results are presented for OC and SC in terms of the motion characteristics and the tension characteristics of the most loaded line. For all cases considered, this was the mooring line in line with the combined wind wave and current direction. The maximum design tension for mooring lines is based on the results obtained during extensive numerical simulations for a variety of environmental conditions based on the time domain simulations according to DNVGL-OS-J103 & J101. Therefore, a reliable estimate of the extreme tension response is required at the earliest stage in the design process to achieve sufficient accuracy in the prediction of the mooring line loads and for further design optimisations. Hydrodynamic coefficients are calculated in WADAM for first-order only, first-order + wave drift and second-order and the comparison of the results of surge and pitch motions and tether tension will be presented in the following.

The results obtained from the numerical simulations described above are therefore presented to investigate the importance of the second-order effects on the motion and tension characteristics. Surge and pitch motion are most critical for the operation of the wind turbine and due to co-linear wave wind and current forces. The other motions such as sway, roll and yaw motion are very small and therefore not presented here.

3.1 MAXIMUM DESIGN TENSION FOR CONCEPT FLOATER AND MOORING

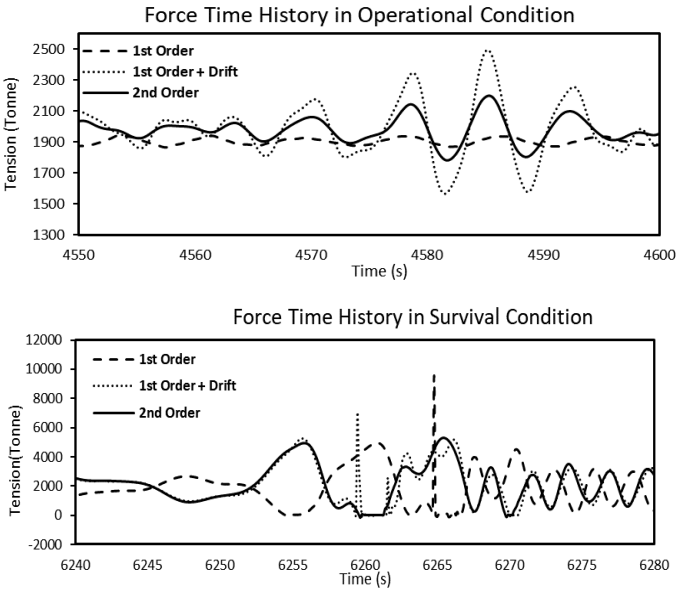

Figure 4: Top Line tension response time series for operating (Top) and survival (Bottom) conditions. Time history shows event around the maximum recorded tension. 2nd Order refers to combined first and second order wave excitation forces.

Figure 4 presents the comparison of the tension response time series of the top mooring line for operation (Top) and survival (Bottom) conditions for the first-order, first-order and drift and complete second-order computations.

Maximum tension values occurring during the three-hour time domain simulation of the operational condition are 2490t, 2495t and 2200t for the first-order, first-order and drift and second-order computations respectively. Average tension recordings are slightly higher for second-order and drift force computations which are due to the mean drift forces acting on the wind turbine. Accounting for second-order effects, the maximum tension response is decreased as can be seen from the standard deviations in Table 4 and Figure 4 (Top) due to the wave drift damping.

The mean tension in the mooring lines remains relatively constant for the operating and survival condition. However, the maximum response and standard deviation increase fourfold.

The tension response in extreme weather shows similar trends for first order, first order + drift and combined first and second order and mean values of the most loaded mooring line are comparable. However, the occurrence of large spikes can be observed for a number of simulations with different wave seeds that do not include the second-order wave effects. These spikes may be due to loss of tension and subsequent snap loads which could be amplified by the application of the static wind force.

Table 4: Force and Motion Response Characteristics in Operational Condition

		Time (s)	Max	Min	Mean	Std.Dv.
1st order	Tension (T)	4585	2490.08	1522.35	1977.51	120.59
	Pitch (Deg.)		0.42	-0.21	0.0942	0.0804
	Surge (m)		0.43	-0.27	0.0688	0.0898
1st Order + Drift	Tension (T)	4585	2495.88	1534.34	1982.56	120.73
	Pitch (Deg.)		0.42	-0.20	0.0981	0.0805
	Surge (m)		0.42	-0.25	0.0726	0.0900
1st order + 2nd Order	Tension (T)	4585	2199.72	1782.21	1978.90	53.61
	Pitch (Deg.)		0.23	-0.03	0.0953	0.0357
	Surge (m)		0.22	-0.07	0.0699	0.0399

3.2 IMPORTANCE OF INCLUSION OF SECOND-ORDER WAVE FORCES

With co-linear wind, wave and current conditions and a constant thrust force acting on the rotor centre, the motion in surge and pitch appear strongly coupled as shown in Figure 5. While the trend of the motion is comparable between the first-order and first order + drift computations, the computations of the complete second-order wave forces reduces the maximum motions in surge and pitch.

Figure 5 presents force and displacement time history while FOWT is operating. It shows that the mooring lines are under the maximum tension at the time the FOWT experienced maximum surge motion.

Table 4 lists the characteristics of force and motion response of the TLB in operational condition. The maximum tension will happen while the maximum surge and pitch motion coupled and occur at the same time. As the other motions are negligibly small this paper only presents maximum value of tensions, surge and pitch motions. Comparison of the values for the first-order, first-order with drift force and second-order effects shows the standard deviation is similar for first-order effects and first-order with drift force effects but it has reduced significantly when considering second-order effects. The mean values have small fluctuation with small differences which remain within less than 5 tonnes.

Maximum tension values are occurring at same time during the three-hour time domain simulation and are 2490t, 2496t and 2200t for the first-order, first-order and drift and second computations respectively. The maximum surge and pitch values decreased while half for second-order effect is considered compared with other two scenarios.

The maximum surge displacements occurring at same time during the three-hour time domain simulation are 0.43m, 0.44m and 0.22m for the first-order, first-order and drift and second computations respectively. The pitch angle is less than half degree in all cases considered. The maximum pitch motions are same for first-order and first-order with drift effect and equal to 0.42°, reduced to 0.23° when considering second-order effects.

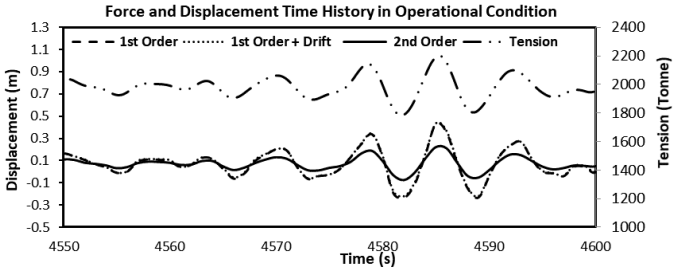

Figure 5: Comparison of surge motions time series of 1st order, 1st order with drift force and 2nd order effects with force time history of 2nd order effect in operational condition. 2nd Order refers to combined first and second order wave excitation forces.

Figure 6 shows strong coupling between surge motion and pitch motion which is also observed for survival conditions. The characteristics of force and motion response of TLB FOWT in survival condition are shown in table 5. For harsh environment conditions, the mean difference between the first-order and second-order solution reduces, however it can be seen that the extreme response peaks are reduced considerably when second-order wave forces are included in the hydrodynamic analysis. The maximum pitch angles in harsh environment with significant wave height of 19.7m are 2.84°, 2.24° and 2.53° for first-order, first-order with drift force and second-order effect computational result respectively.

The maximum pitch angle decreased when including first-order and drift forces and slightly increased for second-order effects. This could be due to appearance of the mean drift force horizontally acting on the floater.

.

Table 5 - Force and Motion Response Characteristics in Survival Condition

		Time (s)	Max	Min	Mean	Std.Dv.
1st order	Tension (T)	6266	9567.25	-149.54	1834.17	571.32
	Pitch (Deg.)		2.84	-2.22	0.0218	0.3307
	Surge (m)		3.20	-0.27	0.0198	0.4331
1st Order + Drift	Tension (T)	6261	7005.59	-130.11	1953.44	592.98
	Pitch (Deg.)		2.24	-3.79	0.0529	0.3324
	Surge (m)		2.65	-4.22	0.0506	0.4347
1st order + 2nd Order	Tension (T)	6266	5300.93	-170.18	1971.64	595.31
	Pitch (Deg.)		2.53	-1.97	0.0748	0.3331
	Surge (m)		2.83	-2.43	0.0689	0.4351

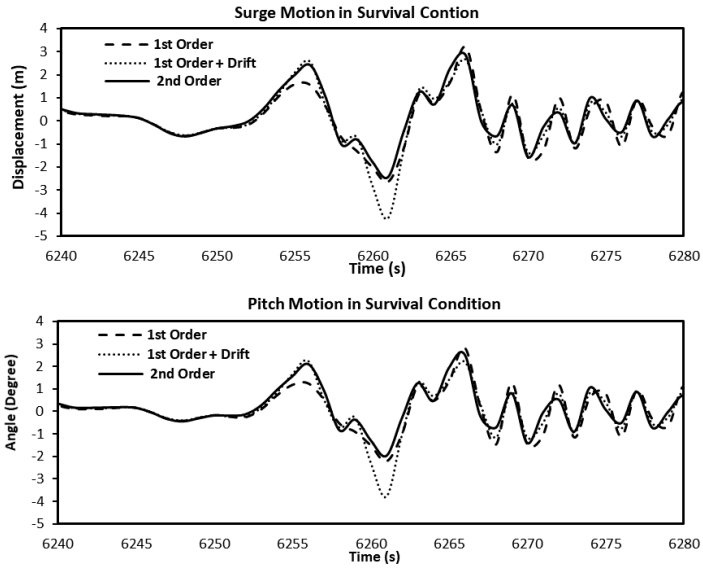

Figure 6:- Comparison of surge (Top) and pitch (Bottom) time series for numerical calculation with 1st order and 2nd order wave force in survival condition (Hs=19.7m Tp=13.2sec). 2nd Order refers to combined first and second order wave excitation forces.

Figure 7 shows the comparison of the time history of the second-order effect computational result of maximum tension with surge displacement of first-order, first-order with drift force and second-order effects computational results

As shown in Figure 7 and **Error! Reference source not found.**, the maximum tension occurs due to coupling of the surge and pitch motions in survival condition. The standard deviation is slightly increased when considering first-order with drift force effects compared to first-order by about 6.5 tonnes. The standard deviation difference between first-order with drift force effect and second-order is small and less than a tonne.

The comparison of the results for the first-order, first-order with drift force and second-order effects has shown the mean value for tension and motions are similar and increased slightly for three cases. Maximum tension values are occurring at the same time during the three-hour time domain simulation and are 9567t, 7006t and 5301t for the first-order, first-order and drift and second computations respectively.

The surge and pitch maximum results decreased when the second-order effect is considered compared with the other two scenarios.

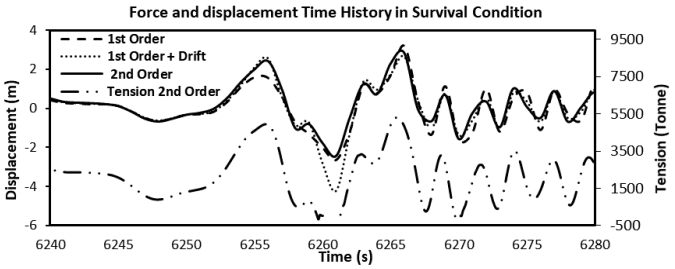

Figure 7: Comparison of surge motions time series of 1st order, 1st order with drift force and 2nd order effects with force time history of 2nd order effect in survival condition. 2nd Order refers to combined first and second order wave excitation forces.

CONCLUSION

This study presented a concept design for TLB FOWT system to support a wind turbine with capacity of 10 MW. The numerical methodology is presented for a coupled hydro-elastic analysis under combined wind, wave and current effect. Platform motion and mooring line tension characteristics are analysed for three-hour time domain solution representing operating and survival conditions in the North Sea with water depth of 110m.

In survival condition mean tension value and standard deviation increased marginally when second-order wave forces and wave drift damping are included in the hydrodynamic analysis. The pitch and surge motions are reduced by 0.31° and 0.37m respectively. For definitive conclusions regarding the occurrence of large spikes, further numerical tests have to be conducted using a larger amount of wave seeds and detailed investigation of the motion and tension time series.

In operational condition the maximum values of the tension, pitch and surge motions are close for first-order and first-order with drift force. However, the maximum tension is reduced by about 12% when accounting for second-order effects. The pitch and surge motions are reduced by 0.19° and 0.20m respectively.

The results of the analysis showed that the effect of including the second-order effects is more significant in survival condition than in the operational conditions.

Since extreme environmental conditions play a vital role in the design of floating offshore wind turbine, the inclusion of second-order effects will improve concept design and lead to more realistic prediction of force and responses at early stages and avoid overdesign of the system due to significant peak responses recorded when only first-order effects are included in the initial analysis. Therefore, the time savings achieved by omitting second-order results are leadings to more design iterations in the design process. Hence, the inclusion of non-linear forces is vital to be considered from the outset.

The TLB FOWT presented in this concept study shows the best overall behaviour considering platform motions in the considered environmental conditions. The preliminary design therefore can be a solution for cost reduction in terms of construction methodology and simplicity of installation procedures compared with other existing FOWT platforms. The results of this study, which uses a coupled nonlinear code, may be used to develop more efficient analysis routines for optimisation and improved design. However, the design optimization and improvement of the concept is still on going and investigation of mooring line tension at fairlead and anchor connection will have to be carried out to provide the optimum solution in terms of simplicity of construction, installation and maintenance.

The reductions in extreme tension values between first and complete second order computations have been recorded in a number of wave time series with varying wave seeds. While this extreme tension response may be a feature of a combination of the TLB characteristics and specific wave series, the trend of tension reductions is presented to highlight the sensitivity of this system's response to the numerical methods chosen in regards to the computation of wave excitation forces. Further testing is currently being undertaken with optimised models that account for the operation and detailed geometry of the wind turbine.

The next stage of this study is to consider in full the aerodynamic effects from rotating turbine on the complete system, include a variety of different environmental conditions and mooring system optimization in terms of anchor radius, number of the lines, elasticity of the mooring line material and connection at fairlead and anchor to investigate the fatigue and horizontal and vertical load at anchor as well as fairlead.

Acknowledgement

The authors would like to express their gratitude to Flintstone Technology Ltd for the financial support for carrying out this research project.

REFERENCES

1. Wind Europe, *Floating Offshore Wind Vision Statement*. 2017.
2. Myhr, A., et al., *Levelised cost of energy for offshore floating wind turbines in a life cycle perspective.* Renewable Energy, 2014. **66**: p. 714-728.
3. EWEA. *Deep water*. 2013 09/10/2018]; Available from: http://www.ewea.org/fileadmin/files/library/publications/reports/Deep_Water.pdf.
4. Carbon Trust. *Floating Wind Joint Industry Project: Policy & Regulatory APPraisal*. 2017 10/10/2018]; Available from: https://www.carbontrust.com/media/673978/wp1-flw-jip-policy-regulatory-appraisal_final_170120_clean.pdf.
5. Witte, T., S. Siegfriedsen, and M. El-Allawy, *WindDeSalter® Technology Direct use of wind energy for seawater desalination by vapour compression or reverse osmosis.* Desalination, 2003. **156**(1-3): p. 275-279.
6. WindFloat. *The WindFloat Project*. 2017 11/10/2018]; Available from: eusew.eu/sites/default/files/programme-additional-docs/WindFloat%20Project%20Update.pdf.
7. Roddier, D., et al. *Summary and Conclusions of the Full Life-Cycle of the WindFloat FOWT Prototype Project*. in *ASME 2017 36th International Conference on Ocean, Offshore and Arctic Engineering*. 2017. American Society of Mechanical Engineers.
8. Statoil. *Statoil to build the world's first floating wind farm: Hywind Scotland*. 2017 15/01/2018]; Available from: https://www.statoil.com/en/news/hywindscotland.html.
9. Nielsen, F.G. *Hywind. Deep offshore wind operational experience*. in *10th Deep Sea Offshore Wind R&D Conference*. 2013.
10. Shin, H. *Model test of the OC3-Hywind floating offshore wind turbine*. in *The Twenty-first International Offshore and Polar Engineering Conference*. 2011. International Society of Offshore and Polar Engineers.
11. Henderson, A., R. Leutz, and T. Fujii, *Potential for floating offshore wind energy in Japanese waters.* 2002.
12. Fukushima Offshore, *Fukushima Floating Offshore Wind Farm Demonstration Project Demonstration Project （Fukushima FORWARD）*. 2014.
13. JWPA. *Offshore Wind Power Development in Japan*. 2017 12/10/2018]; Available from: http://jwpa.jp/pdf/20170228_OffshoreWindPower_inJapan_r1.pdf.
14. Matha, D., et al., *Efficient preliminary floating offshore wind turbine design and testing methodologies and application to a concrete spar design.* Phil. Trans. R. Soc. A, 2015. **373**(2035): p. 20140350.
15. Athanasia Arapogianni, a.A.-B.G.E., the members of the European and W.E.A.s.E.O.W.I.G. (OWIG), *Deep Water-The next step for offshore wind energy*. 2013.
16. GL Garrad Hassan. *A Guide to UK Offshore Wind Operations and Maintenance*. 2013 0/10/2018]; Available from: http://www.hi-

energy.org.uk/Downloads/General%20Documents/guide-to-uk-offshore-wind-operations-and-maintenance.pdf.
17. BIS Group. *The Challenges Offshore Wind Faces on the way to Renewable and Clean Energy*. 2016 9/10/2018]; Available from: http://www.offshorewindindustry.com/news/challenges-offshore-wind-faces-way-to.
18. Carbon Trust, *Floating Offshore Wind: Market and Technology Review* 2015.
19. Sclavounos, P., C. Tracy, and S. Lee. *Floating offshore wind turbines: Responses in a seastate pareto optimal designs and economic assessment*. in *ASME 2008 27th International Conference on Offshore Mechanics and Arctic Engineering*. 2008. American Society of Mechanical Engineers.
20. Myhr, A., *Developing offshore floating wind turbines: the Tension-Leg-Buoy design.* 2016.
21. Myhr, A., K.J. Maus, and T.A. Nygaard. *Experimental and computational comparisons of the OC3-HYWIND and Tension-Leg-Buoy (TLB) floating wind turbine conceptual designs*. in *The Twenty-first International Offshore and Polar Engineering Conference*. 2011. International Society of Offshore and Polar Engineers.
22. Bak, C., et al. *The DTU 10-MW reference wind turbine*. in *Danish Wind Power Research 2013*. 2013.
23. Pegalajar-Jurado, A., H. Bredmose, and M. Borg, *Multi-level Hydrodynamic Modelling of a Scaled 10MW TLP Wind Turbine.* Energy Procedia, 2016. **94**: p. 124-132.
24. Bredmose, H., et al. *Experimental study of the DTU 10 MW wind turbine on a TLP floater in waves and wind*. in *EWEA Offshore Conference, Copenhagen, Denmark, Mar*. 2015.
25. Skaare, B., et al., *Analysis of measurements and simulations from the Hywind Demo floating wind turbine.* Wind Energy, 2015. **18**(6): p. 1105-1122.
26. Roald, L., et al., *The effect of second-order hydrodynamics on floating offshore wind turbines.* Energy Procedia, 2013. **35**: p. 253-264.
27. Veritas, D.N., *Wave analysis by diffraction and morison theory (Wadam).* SESAM User's Manual, Det Norske Veritas (DNV): Høvik, Norway, 1994.
28. Lee, C.-H. and J. Newman, *Computation of wave effects using the panel method.* WIT Transactions on State-of-the-art in Science and Engineering, 2005. **18**.
29. Nuernberg, M. and L. Tao, *Coupled Hydrodynamic Analysis of Floating Offshore Wind Turbine Support Structures*, in *International Maritime Conference on Design for Safety*. 2013: Shanghai.
30. Roald, L., J. Jonkman, and A. Robertson, *The Effect of Second-Order Hydrodynamics on a Floating Offshore Wind Turbine*. 2014, National Renewable Energy Laboratory (NREL): www.nrel.gov/publications. p. 156.
31. Islam, M.T., *Design, Numerical Modelling and Analysis of a Semi-submersible Floater Supporting the DTU 10MW Wind Turbine*. 2016, NTNU.
32. Bak, C., et al., *Description of the DTU 10 MW Reference Wind Turbine. 2013.* DTU Vindenergi, 2013.
33. George, J., *WindFloat design for different turbine sizes.* Master's Thesis Project, Instituto Superior Técnico Technical University of Lisbon, Portugal, MS, 2014.
34. Trolle, J. and F. Hornbak, *Optimization of Tension Leg Buoy with regards to Stabilization Failure*, in *Department of Civil Engineering*

Division of Structures, Materials and Geotechnics. 2016, Aalborg University Esbjerg

Esbjerg, Denmark.
35. Orcaflex. *Rope/wire: Axial and bending stiffness*. 2015 06/09/2018]; Available from: https://www.orcina.com/SoftwareProducts/OrcaFlex/Documentation/Help/Content/html/Ropewire,Axialandbendingstiffness.htm.
36. Al-Solihat, M.K. and M. Nahon, *Stiffness of slack and taut moorings.* Ships and Offshore Structures, 2016. **11**(8): p. 890-904.
37. Roddier, D., et al., *WindFloat: A floating foundation for offshore wind turbines.* Journal of renewable and sustainable energy, 2010. **2**(3): p. 033104.
38. ORECCA-RSE, *Off-shore Renewable Energy Conversion platforms - Coordination Action*. 2018.